Applied Geography 151 (2023) 102853

Contents lists available at ScienceDirect

Applied Geography

journal homepage: www.elsevier.com/locate/apgeog

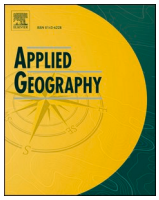

Supply and demand dynamics of hydrologic ecosystem services in the rapidly urbanizing Taihu Lake Basin of China

Yu Tao [a,b,c,1], Zhaobi Li [d,1], Xiao Sun [e], Jiangxiao Qiu [c], Steven G. Pueppke [f,g], Weixin Ou [a,b,*], Jie Guo [a,b], Qin Tao [a], Fei Wang [a]

[a] College of Land Management, Nanjing Agricultural University, Nanjing, 210095, China
[b] National & Local Joint Engineering Research Center for Rural Land Resources Use and Consolidation, Nanjing, 210095, China
[c] School of Forest, Fisheries, and Geomatics Sciences, Fort Lauderdale Research and Education Center, University of Florida, Davie, FL, 33314, USA
[d] Shenzhen Urban Planning and Development Research Center, Shenzhen, 518034, China
[e] Institute of Agricultural Resources and Regional Planning, Chinese Academy of Agricultural Sciences, Beijing, 100081, China
[f] Asia Hub for Water-Energy-Food Nexus, Nanjing, 210095, China
[g] Center for Global Change and Earth Observations, Michigan State University, East Lansing, MI, 48824, USA

ARTICLE INFO

Keywords:
Hydrologic ecosystem services
Water purification
Flood mitigation
Supply and demand
Land use change
Urban expansion

ABSTRACT

Although it is challenging to integrate supply and demand to comprehensively understand urbanization effects on ecosystem services, this knowledge is essential, especially in rapidly urbanizing areas. A spatially explicit approach was developed here to synthesize supply and demand dynamics of the two most important hydrologic services in the rapidly urbanizing Taihu Lake Basin (TLB) of eastern China. The supply of water purification (WP_S) and flood mitigation (FM_S) were measured as nitrogen removal and runoff retention, respectively. Whereas the demand for water purification (WP_D) was quantified as the difference between total and permitted nitrogen loading based on relevant water quality standards, the demand for flood mitigation (FM_D) was estimated as the vulnerability to potential flood damage, including economic losses and causalities. We found a spatial mismatch where high WP_S and FM_S occurred in mountainous areas while high WP_D and FM_D concentrated in urban and agricultural areas across the basin. WP_S and WP_D decreased by 10% and 20%, respectively during 2000–2015, due mainly to loss of croplands to urban expansion. This was also the main cause of decreased FM_S by 7% but increased FM_D by 67%, which underscored the importance of conserving croplands in rapidly urbanizing regions of the TLB. Overall, land use composition had strong associations with WP_D ($r^2 \geq 0.57$) and FM_S ($r^2 \geq 0.38$) at the sub-basin scale, while the configuration of multiple land uses, such as urban sprawl, cropland fragmentation, and riparian buffers were crucial in influencing WP_S. In comparison, FM_D was most sensitive to urban expansion ($r^2 = 0.74$), economic development ($r^2 = 0.81$), and population growth ($r^2 = 0.93$). These findings provide new insights into sustainable land management for coordinating supply of and demand for hydrologic services in the TLB and other urbanizing watersheds of the world.

1. Introduction

Ecosystem services (ES) supply refers to the products and benefits that nature generates and delivers to humans (Daily et al., 2000), while the demand for ES can be defined as the amount of services consumed, desired or favored by human society (Baró et al., 2016). Measuring the gaps (e.g., spatial, social, functional or institutional) between supply and demand is fundamental to optimizing the flow of ES (Chen et al., 2020) for ecosystem stewardship (Pan et al., 2021) and human well-being (Huang et al., 2020). Unlike the supply of ES, which can be easily quantified with a number of modeling tools, the demand for ES has only recently been investigated due to data gaps and lack of methods (Tao et al., 2018, 2022). Integration of urban intensity, population density, and GDP per capita via the land development index is one of the simplest ways to assess ES demand (Xu et al., 2021; Zhai et al., 2020). In contrast, Li et al. (2020) explored a multi-criteria spatial approach for mapping ES

* Corresponding author. College of Land Management, Nanjing Agricultural University, Nanjing, 210095, China.
E-mail addresses: taoyu@njau.edu.cn (Y. Tao), owx@njau.edu.cn (W. Ou).

[1] These authors contributed equally to this work. Author contributions: Y. Tao and Z. Li designed and performed research; Z. Li and Y. Tao analyzed data; and Y. Tao wrote and revised the paper.

https://doi.org/10.1016/j.apgeog.2022.102853
Received 25 May 2021; Received in revised form 22 November 2022; Accepted 15 December 2022
Available online 20 December 2022

demand in urban areas. The areas with high demand for regulatory and cultural services were identified through GIS analyses of ecological sensitivity, spatial accessibility, and population distribution.

The demand for ES can also be expressed in terms of the preference and expected levels of stakeholders such as local residents and tourists (Wei et al., 2018). This requires a participatory approach involving questionnaire surveys and interviews with stakeholders to gain their perceptions of the importance of ES (Xu et al., 2020). In addition, Burkhard et al. (2012) developed a map-based matrix to directly link multiple land uses with ES demand. The score of each land use ranges from 0 to 5 in each matrix and indicates low to high levels of demand for a specific ES. Thus the total demand for ES can be estimated by adding up the score of every land use pixel in the region. This method enables quick assessment of ES with explicit implications for land management, and it has been employed to quantify ES supply and demand dynamics in response to land use change across mainland China (Wu et al., 2019) and the United States (Sun et al., 2020). However, the above-mentioned methods either rely on expert knowledge for qualitative assessment, or they represent ES demand with socioeconomic indicators that are not comparable to the biophysical indicators of ES supply, making it difficult to precisely quantify the gaps between supply and demand.

Addressing this issue requires quantification of ES demand in accordance with ES supply. This can be straightforward for provisioning services by estimating the direct consumption or use of ecosystem products (Kroll et al., 2012). For instance, the demand for food production was estimated based on total population and per capita food consumption (Cui et al., 2019; Shi et al., 2020), while the demand for water provision was equal to the consumption of water resources from agricultural, industrial, domestic, and environmental sectors (Lin et al., 2021; Ma et al., 2019). In comparison, the demand for regulatory services can be estimated as the amount of regulation needed to comply with environmental quality standards and policy goals (Baró et al., 2015). Chen et al. (2019) calculated the demand for air purification as the difference between the actual concentration of air pollutants and the permitted concentration set by the local government. They also calculated the demand for carbon sequestration by comparing carbon emissions against carbon reduction targets, which can be set either by government agencies or determined based on climate assessment. In several other studies, the demand for sediment and nutrient retention was estimated as soil erosion and nutrient loading (Hou et al., 2020; Pan et al., 2021), but these estimates should be ideally assessed against water quality standards. In addition, the demand for flood mitigation has been expressed as potential flood damage (Stürck et al., 2015), but the results become valuable only when accurate information on the distribution of assets and population and the depth-damage functions are adjusted for the local region.

On the basis of these quantitative methods, researchers were able to further integrate ES demand with supply to identify mismatches across space and over time, especially in rapidly urbanizing regions. As revealed by González-García et al. (2020) and Shi et al. (2020), the supply/demand ratios of several provisioning, regulatory, and cultural services increased along the respective urban-rural gradients of Shanghai and Madrid. The ES deficit area (i.e., demand exceeding supply) also increased as these two metropolises expanded. These results imply that there are notable impacts of urban expansion on both supply and demand of multiple ES. Nonetheless, most of the current studies only assessed the impact of urban expansion on ES supply, because it is more directly linked to land use change (Peng et al., 2017). ES demand nevertheless has more complex interactions with land use and socioeconomic factors in urbanizing regions (Peng et al., 2020), an issue that warrants detailed analysis.

To address these knowledge gaps, this study takes the rapidly urbanizing Taihu Lake Basin (TLB) of China as an example and aims to (1) develop models to quantify the spatial mismatches between supply and demand of two primary hydrologic ecosystem services (i.e., water purification and flood mitigation) in the basin; (2) characterize the supply and demand dynamics of these two ES in response to rapid urban expansion; and (3) evaluate land use effects to formulate land management strategies for coordination of ES supply and demand.

2. Materials and methods

2.1. Study area

The TLB is located in the core area of the Yangtze River Delta in eastern China (119°3′1″-121°54′26″E, 30°7′19″-32°14′56″N). It covers an area of approximately 36,900 km^2, which is bounded by the Qiantang River to the south, the Yangtze River to the north, the East China Sea to the east, and the Maoshan and Tianmu Mountains to the west (Fig. 1). The basin lies within the subtropical monsoon climate zone, with an annual mean temperature of 15–17 °C and annual mean precipitation of 1010–1400 mm. The TLB has a complex surface water system with over 200 rivers and 10 lakes that are larger than 10 km^2. Lying in the heart of the basin, Taihu Lake is the third largest freshwater lake in China with an area of 2428 km^2. The terrain of the TLB is characterized by alluvial plains that cover more than two-thirds of its area and low mountains mostly in the southwest. Owing to its flat terrain and favorable climate, the TLB is one of the most agriculturally productive regions in China. The paddy fields that make up about half of the basin area are the major sources of nutrients and pollutants discharged into open water bodies.

The TLB includes Shanghai and parts of Jiangsu, Zhejiang, and Anhui provinces, and it is also one of the most populous and economically developed regions in the country. By 2020, the basin supported 4.8% of the nation's population and produced 9.8% of its GDP with only 0.4% of the total land area in China (Taihu Basin Authority of Ministry of Water Resources, 2020). As of 2015, urban land occupied more than one fourth of the basin territory after a fifteen-year consecutive expansion by 3.4% annually since 2000 (Fig. 1). The combination of continuing rapid urbanization and agricultural intensification poses serious challenges for the regulation of water quantity and quality in the TLB. According to the Health Status Report of Taihu Lake (Taihu Basin Authority of Ministry of Water Resources, 2015), recent floods are occurring more frequently and with a much broader impact than was the case decades ago. In 2015, more than half of the surface water area in the TLB, as well as 13 of the 22 rivers that directly drain into Taihu Lake failed to meet the national water quality standard for excessive amounts of nitrogen and phosphorus. As a result, algal blooms spread over half of the lake's area in 2015.

2.2. Data sources

Six major datasets were used in this study. (1) Land use and land cover data (30-m resolution) for the TLB between 2000 and 2015 were produced by the Institute of Remote Sensing and Digital Earth, Chinese Academy of Sciences through interpretation of Landsat TM or ETM images. Land uses in the TLB were classified into nine categories, including high density urban, low density urban, unused land, paddy field, rainfed cropland, grassland, woodland, wetlands, and open water (Fig. 1). The overall accuracy of classification relative to the ground-based survey data was over 85% (Liu et al., 2014). (2) Mean annual precipitation and evapotranspiration data (1-km resolution) during the years 2000–2015 were obtained by spatial interpolation of rainfall observations from the National Ecosystem Science Data Center (http://rs.cern.ac.cn/). (3) The topographic map (30-m resolution) and soil map (1-km resolution) for the TLB were derived from the China Geospatial Data Cloud (www.gscloud.cn) and the Harmonized World Soil Database (HWSD) for sub-basin delineation and hydrological modelling, respectively. (4) The boundaries of the 490 sub-basins were delineated by the Nanjing Institute of Geography and Limnology, Chinese Academy of Sciences in two major steps. First, the TLB was divided into sub-basins using DEM data (30-m resolution) and the SWAT tool. Second, the boundaries of these sub-basins were further corrected (e.g., merged,

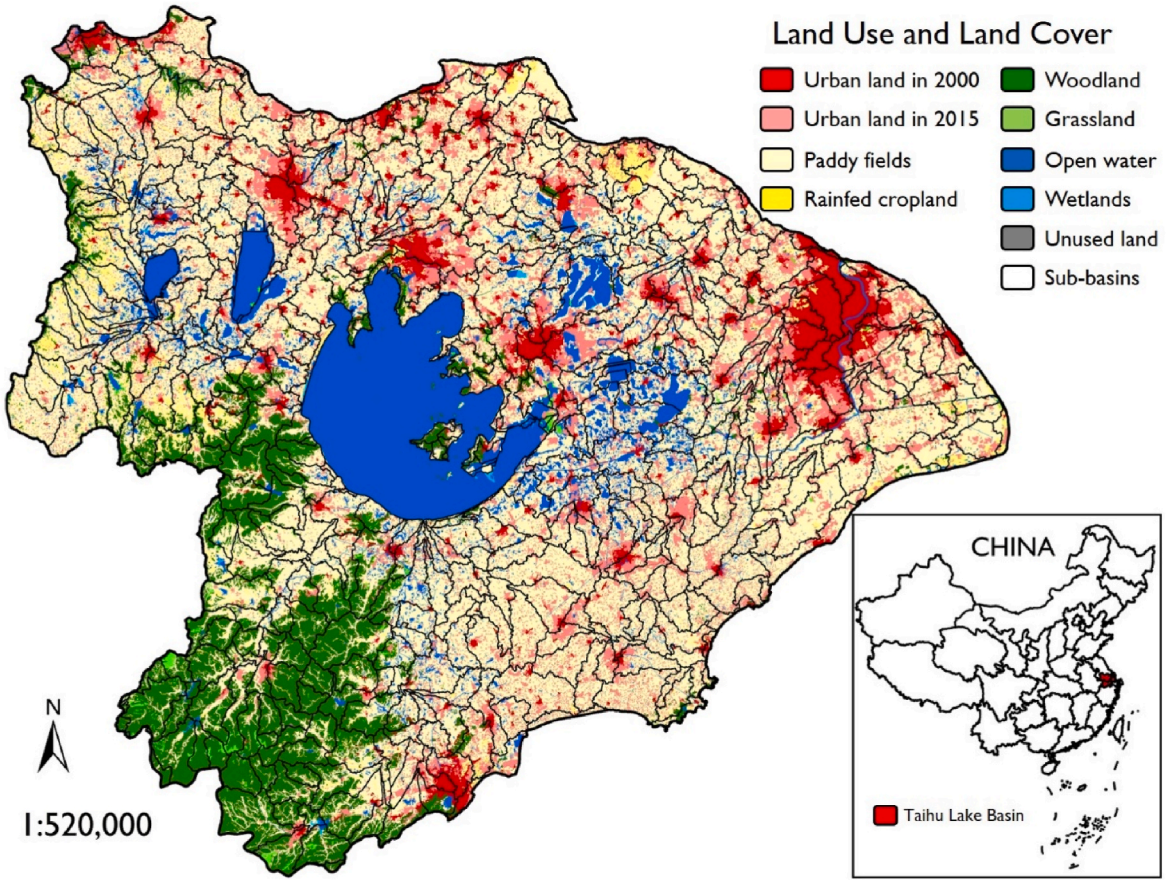

Fig. 1. Geographical location and land use/land cover of the Taihu Lake Basin in 2015.

segmented, or reshaped) manually in the ArcGIS software based on the distribution of ditches, dikes, and dams in the TLB. (5) The gridded GDP and population products (1-km resolution) for the years 2000 and 2015 were produced based on urban density, nighttime lights, and county-level statistics by the Data Center for Resources and Environmental Sciences, Chinese Academy of Sciences (http://www.resdc.cn/). (6) The biophysical variables used in the ecosystem service models, such as plant evapotranspiration, runoff coefficient, nitrogen export and retention efficiency of different land uses (Table 1), were derived from field studies conducted in the TLB (Wen et al., 2011; Xu et al., 2017).

Table 1
Biophysical parameters in the runoff and nitrogen retention models.

LULC	Kc	root_depth	load_n	eff_n	LULC_veg	CN_2
High intensity urban	0.1	100	9.87	0.05	0	90
Low intensity urban	0.2	200	8.39	0.05	0	80
Unused land	0.3	300	6.81	0.05	0	70
Paddy field	1.1	2000	33.60	0.25	0	60
Rainfed cropland	0.7	2000	21.80	0.25	1	50
Grassland	0.6	2000	5.33	0.4	1	40
Woodland	1	7000	3.57	0.8	1	20
Wetlands	1.2	2000	2.35	0.5	0	30
Open water	1	1000	0.01	0.05	0	100

Note: Kc = plant evapotranspiration coefficient; root_depth = maximum root depth (mm) for vegetated land use types; load_n = annual nitrogen loading ($kg{\cdot}ha^{-1}$); eff_n = maximum nitrogen retention efficiency; LULC_veg: = 1 for vegetated land use types except wetlands, and 0 for all other land use types; CN_2 = curve number.

2.3. Assessing water purification supply and demand

2.3.1. Water purification supply

In this study, the supply of water purification service (WP_S) refers to the capacity of terrestrial ecosystems to retain and intercept non-point sourced nitrogen exported primarily from agricultural and urban areas to the water bodies (Hoyer & Chang, 2014). Accordingly, WP_S was measured as the proportion of nitrogen retention to total nitrogen loading in each sub-basin of the TLB. This was quantified using the InVEST nitrogen retention model (Sharp et al., 2018) as follows:

$$WP_S = \left(1 - \frac{\sum Exp_x}{\sum ALV_x}\right) \bullet 100\%$$

where $\sum \mathrm{Exp}_x$ is the total amount of nitrogen exported from any upstream grid cell x within a sub-basin that eventually reaches downstream water bodies, and $\sum ALV_x$ is the sum of nitrogen loading from all grid cells within a sub-basin.

$$Exp_x = ALV_x \prod_{y=x+1}^{X} \left(1 - R_y\right)$$

where R_y is the nitrogen retention efficiency of each downstream grid cell y, and X represents the number of downstream grid cells.

$$ALV_x = HSS_x \bullet pol_x$$

where pol_x is the export coefficient for grid cell x, and HSS_x is the hydrological sensitivity score for grid cell x. The nitrogen export coefficient and retention efficiency for different land use types in the TLB were derived as described previously (Li et al., 2013; Wang et al., 2017; Wen et al., 2011) and are shown in Table 1.

$$HSS_x = \frac{\lambda_x}{\overline{\lambda_B}}$$

where λ_x is the runoff index for grid cell x, and $\overline{\lambda_B}$ is the mean runoff index in the TLB.

$$\lambda_x = \log \sum_U Y_u$$

where $\sum_U Y_u$ is the total water yield of grid cells along the flow path above grid cell x. Water yield was estimated on the basis of mean annual precipitation between 2000 and 2015.

2.3.2. Water purification demand

The demand for water purification service (WP_D) refers to the amount of nitrogen that ought to be retained and intercepted before entering the water bodies in order to maintain surface water quality standards (Wang et al., 2019). WP_D was measured by comparing the total nitrogen loading (ALV_{load}) of a sub-basin to its allowable amount of nitrogen export (Exp_{allow}) based on a referenced water quality standard (Fig. 2).

$$WP_D = \begin{cases} 0, if\ ALV_{load} \le Exp_{allow} \\ \frac{ALV_{load} - Exp_{allow}}{ALV_{load}} \bullet 100\%, if\ ALV_{load} > Exp_{allow} \end{cases}$$

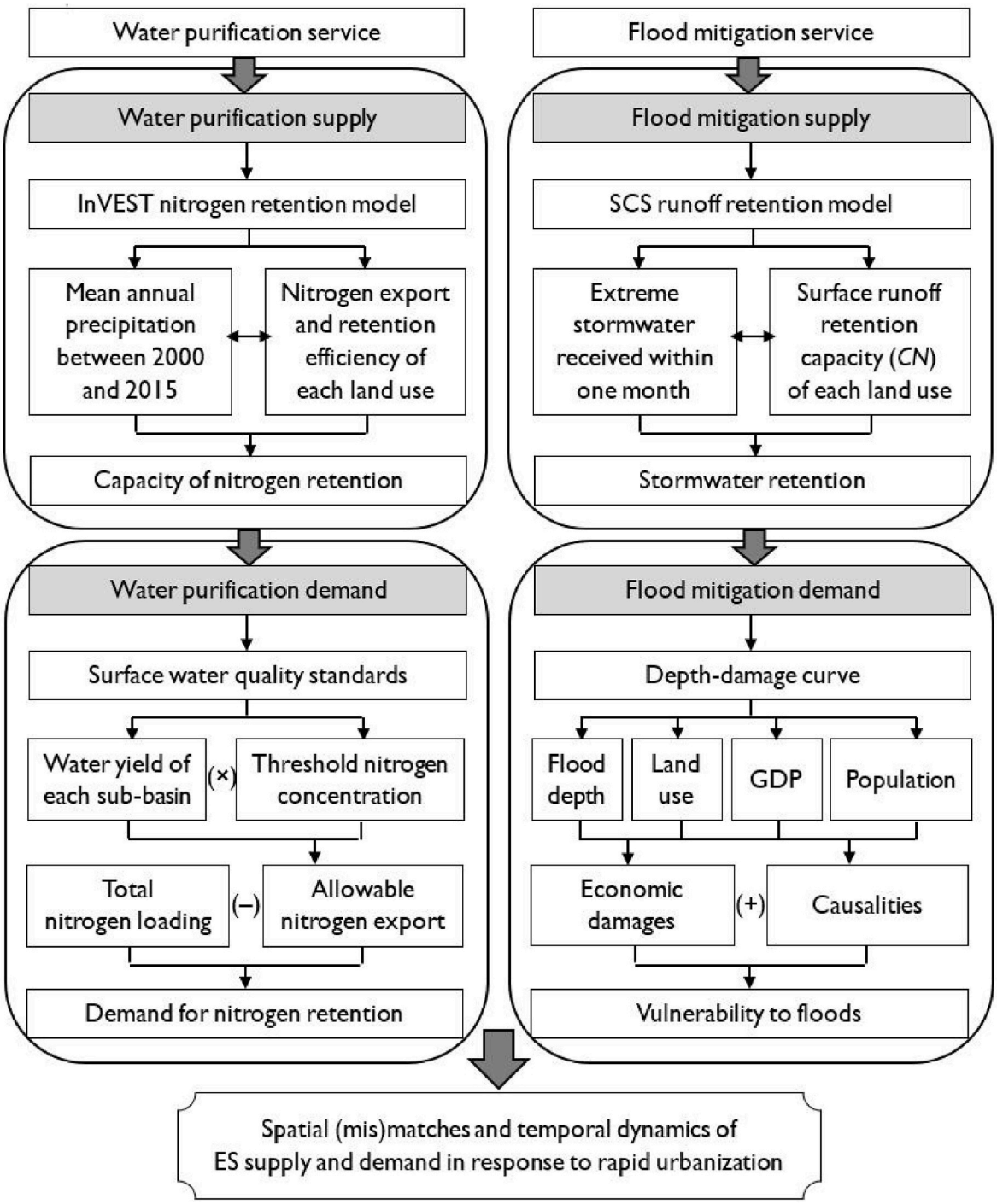

Fig. 2. Research framework to integrate supply and demand of hydrologic ecosystem services.

Exp_{allow} was further estimated as follows:

$$Exp_{allow} = \sum Y_x \bullet \rho$$

where $\sum Y_x$ is the total water yield of a sub-basin, and ρ is the threshold concentration of nitrogen in the runoff. In this study, ρ was set to a value of 1 g/m^3, which corresponds to the national water quality standard of China.

2.4. Assessing flood mitigation supply and demand

2.4.1. Flood mitigation supply

The supply of flood mitigation service (FM_S) refers to the capacity of terrestrial ecosystems to retain stormwater and reduce quick flow during the rainy season (Shen et al., 2021). FM_S was measured here as the proportion of runoff retention to total precipitation in each sub-basin of the TLB. This was quantified using the SCS runoff retention model (Shi et al., 2001) as follows:

$$FM_S = \left(1 - \frac{Q}{P}\right) \bullet 100\%$$

where Q indicates the amount of surface runoff (or quick flow), and P is total precipitation during the rainy season. Based on historical observations from rainfall stations, P was set as 600 mm in one month or less as an indicator of extreme precipitation conditions.

$$Q = \begin{cases} \dfrac{(P - 0.2S)^2}{P + 0.8S}, if\ P \geq 0.2S \\ 0, if\ P < 0.2S \end{cases}$$

where S indicates the maximum runoff retention capacity (mm) of a grid cell.

$$S = \frac{25400}{CN_{2s}} - 254$$

where CN_{2S} is the adjusted curve number that indicates the influence of terrain, land use, and soil texture and moisture on runoff generation. It was estimated using the slope of each grid cell as follows:

$$CN_{2s} = \frac{(CN_3 - CN_2)}{3} \bullet [1 - 2 \bullet exp(-13.86 \bullet slope)] + CN_2$$

$$CN_3 = CN_2 \bullet exp[0.00673 \bullet (100 - CN_2)]$$

The curve number (CN_2) of different land use types in the TLB were derived as described previously (Peng et al., 2018; Xu et al., 2017) and are shown in Table 1.

2.4.2. Flood mitigation demand

The demand for flood mitigation service (FM_D) was quantified based on the vulnerability of a sub-basin to flood damage (Stürck et al., 2014). Specifically, the degree of vulnerability was measured as the losses of two most important assets – gross domestic product (GDP) and human lives caused by floods (Fig. 2). Accordingly, FM_D was determined with the following equation:

$$FM_D = \frac{\overline{GDP_{loss}} + \overline{POP_{loss}}}{2} \bullet 100\%$$

where $\overline{GDP_{loss}}$ and $\overline{POP_{loss}}$ are the average losses of GDP and human lives in all grid cells of a sub-basin. Both indices were rescaled to the range between 0 and 1 through linear normalization. This facilitated direct comparison and integration. For each grid cell, GDP_{loss} and POP_{loss} were estimated as follows:

$$GDP_{loss} = GDP \bullet D(h)$$

$$POP_{loss} = POP \bullet M(h)$$

$$D(h) = \begin{cases} 0.461h - 0.051h^2, for\ urban\ land \\ 0.335h - 0.029h^2, for\ cropland \end{cases}$$

$$M(h) = e^{\frac{h-5.78}{0.82}}$$

where GDP and POP represent the total gross domestic product and population, respectively, in each grid cell. h is the flood depth measured as surface runoff in meters. $D(h)$ and $M(h)$ are the damage rate and mortality rate estimated on the basis of flood depth-damage functions for Asian countries (Huizinga et al., 2017; Jonkman, 2007).

2.5. Quantifying spatial matches and mismatches between ES supply and demand

Owing to inconsistent units of measurement for ES supply and demand, we compared ES supply with demand by grouping all the 980 sub-basins of the TLB into nine categories based on their rankings in ES supply and demand over 2000–2015. Following Qiu and Turner (2013) and Shen et al. (2019), the highest ranked 20% of the sub-basins were then designated as high in supply (or demand), the bottom ranked 20% as low in supply (or demand), and the middle ranked 60% as moderate in supply (or demand). The spatial matches and mismatches between ES supply and demand could consequently be represented with a 3 × 3 color matrix that differentiated the nine possible relationships. As shown in Fig. 3*f* and 4*f*, for instance, the HL type indicates a sub-basin with high supply and low demand, and vice versa. We also conducted *OLS*-based nonlinear fitting analyses to understand the spatial variations of ES supply and demand in response to differences in land use and urbanization at the sub-basin scale. Here, the level of demographic, economic, and spatial urbanization was measured by population density, GDP per area, and proportion of urban land, respectively (Peng et al., 2020). Technically, population density (or GDP per area or proportion of urban land) of each sub-basin was estimated as the sum of population (or GDP or urban area) from every grid cell within each sub-basin divided by the area of each sub-basin.

3. Results

3.1. Spatio-temporal variations of water purification supply and demand

We estimated that the total nitrogen loading in the TLB amounted to 77,860 tons in 2000 and 69,508 tons in 2015; the corresponding figures for nitrogen retention were 58,963 tons in 2000 and 53,242 tons in 2015. Accordingly, the supply of water purification (WP_S) as measured by nitrogen retention efficiency, was about 75% in both years for the basin as a whole, but as shown in Fig. 3*a* and 3*b*, WP_S varied significantly depending on location. WP_S was lower than 75% in less than 10% of the basin territory as of 2000, but the proportion of area with WP_S lower than 75% had grown to 24% by 2015. The increase in this category was primarily due to urban expansion (65% increase), which encroached onto croplands (16% decrease) and wetlands (8% decrease), resulted in decreased nitrogen retention efficiency (Table 1). In comparison, WP_S was between 75 and 85% in more than 80% of the basin territory, and these regions shrank by only 2% between 2000 and 2015.

Reduction of nitrogen to the allowable standard of ≤1 g/m^3 of the basin water corresponds to estimated amounts of nitrogen carried in the annual water yield of 27,155 tons in 2000 and 28,941 tons in 2015. By comparing the differences between these estimates and total nitrogen loading in the basin, we were able to estimate the demand for water purification (WP_D) as the proportion of total nitrogen loading that needed to be reduced in order to bring the TLB into compliance with the standard. This amounted to 65% in 2000 and 58% in 2015. As shown in Fig. 3*c* and 3*d*, WP_D was higher than 70% in nearly half of the basin territory as of 2000, but after an annual decrease of 5% over the past 15 years, these regions of high demand covered only 22% of the total area

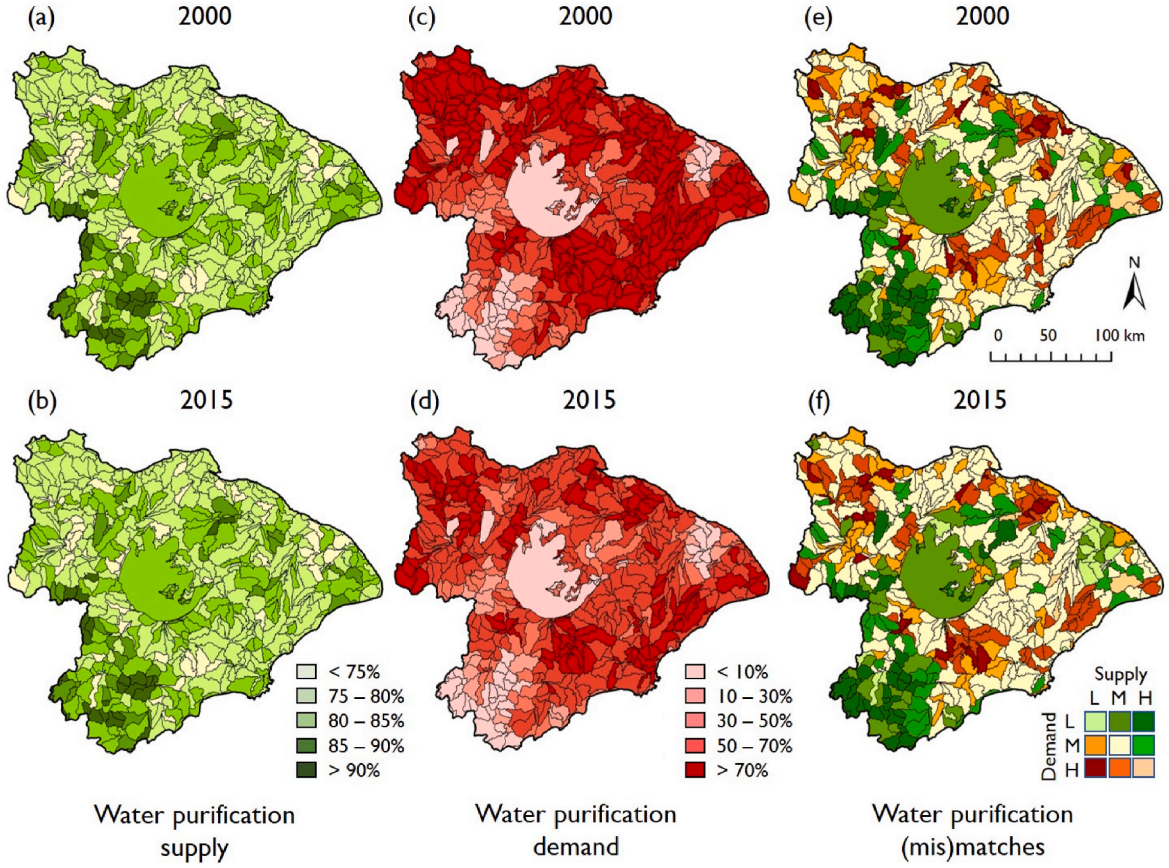

Fig. 3. Water purification supply and demand in 2000 and 2015 (L = low, M = medium, H = high).

in 2015. The decrease in WP_D can be explained by loss of croplands due to urban expansion, which resulted in an 11% decrease in nitrogen loading and a 7% increase in water yield due to changes in biophysical parameters of runoff and nitrogen retention (Table 1). In contrast, the regions of moderate to low demand ($WP_D < 70\%$) accounted for 52% and 78% of the total area in 2000 and 2015, respectively, representing an increase of 3% annually.

Fig. 3*e* and 3*f* map the relationship between water purification supply and demand in the TLB. Regions of high supply are indicated by green to dark green colors and were mostly in the southwest part of the basin and in large water bodies, but regions of high demand, as indicated by red to dark brown colors, were widely dispersed across other areas of the basin. Four regions characterized by high or low supply and high or low demand can be recognized and are designated HH, HL, LH, and LL with respect to supply/demand (Fig. 3*e* and 3*f*). HL regions are indicated by the dark green color and accounted for just 7–8% of the total area. Land areas in this category were located in the low mountains of the southwest part of the basin and contained only 3–4% of the basin total population. In contrast, LL regions, as indicated by the lime green color, were primarily located in Shanghai, Wuxi and surrounding urban areas. These regions were densely populated, with 12–14% of the total population in only 2–3% of the basin territory. As hotspots for nitrogen pollution, the LH regions, as indicated by dark brown, were dominated by croplands, but the HH regions, as indicated by light brown, were comprised of croplands and woodland with high nitrogen loading and high retention efficiency. In total, the HL, LL, LH, and HH regions covered 15% of the total area and contained 20% of the total population of the TLB during 2000–2015.

3.2. Spatio-temporal variations of flood mitigation supply and demand

In this analysis, the TLB received 17.43 billion cubic meters of storm water within one month of the rainy season. As a result, the entire basin generated 12.9 and 13.2 billion cubic meters of surface runoff with land uses in 2000 and 2015, respectively. Thus, the volume of runoff retention amounted to 26% and 24% of the storm water received in the two years, which represented a slight decrease of 7% in the supply of flood mitigation (FM_S) between 2000 and 2015. As shown in Fig. 4*a* and 4*b*, the regions of low supply ($FM_S < 20\%$) expanded from 30% to 53% of the basin territory between 2000 and 2015. This is equivalent to a rapid 5% annual increase and can be attributed to urbanization. Moreover, although FM_S was between 20% and 25% in 42% of the basin area in 2000, the extent of these regions of moderate supply was nearly halved by 2015, when they covered only 22% of the basin. In contrast, the regions of high supply ($FM_S > 25\%$) covered about one quarter of the total area and remained relatively stable between 2000 and 2015.

We estimated a total of 1149 deaths in 2000 and 1636 deaths in 2015 due to extreme flood events in the TLB. The total estimated loss of GDP amounted to 2.5 billion yuan in 2000 and 16.3 billion yuan – more than a six-fold increase – as of 2015. The overall vulnerability score to flood damage, which indicates the demand for flood mitigation (FM_D), averaged 3–5% for the basin, but varied significantly across sub-basins (Fig. 4*c* and 4*d*). Regions of low demand ($FM_D < 4\%$) dominated the TLB, but their area shrank by 31% between 2000 and 2015. In comparison, the regions of moderate to high demand ($FM_D > 4\%$) covered 39% of the basin in 2015 after an 8% annual increase. These significant increases could be attributed to the expansion of densely populated urban areas with rapid economic growth. These urban areas were most vulnerable to flood damages and thus had high demand for flood mitigation.

As shown in Fig. 4*e* and 4*f*, supply of flood mitigation, as indicated by darker green colors, tended to decrease from southwest to northeast in the basin, with a corresponding increase in demand for flood mitigation, as indicated by reddish-brown and brown colors. Four regions

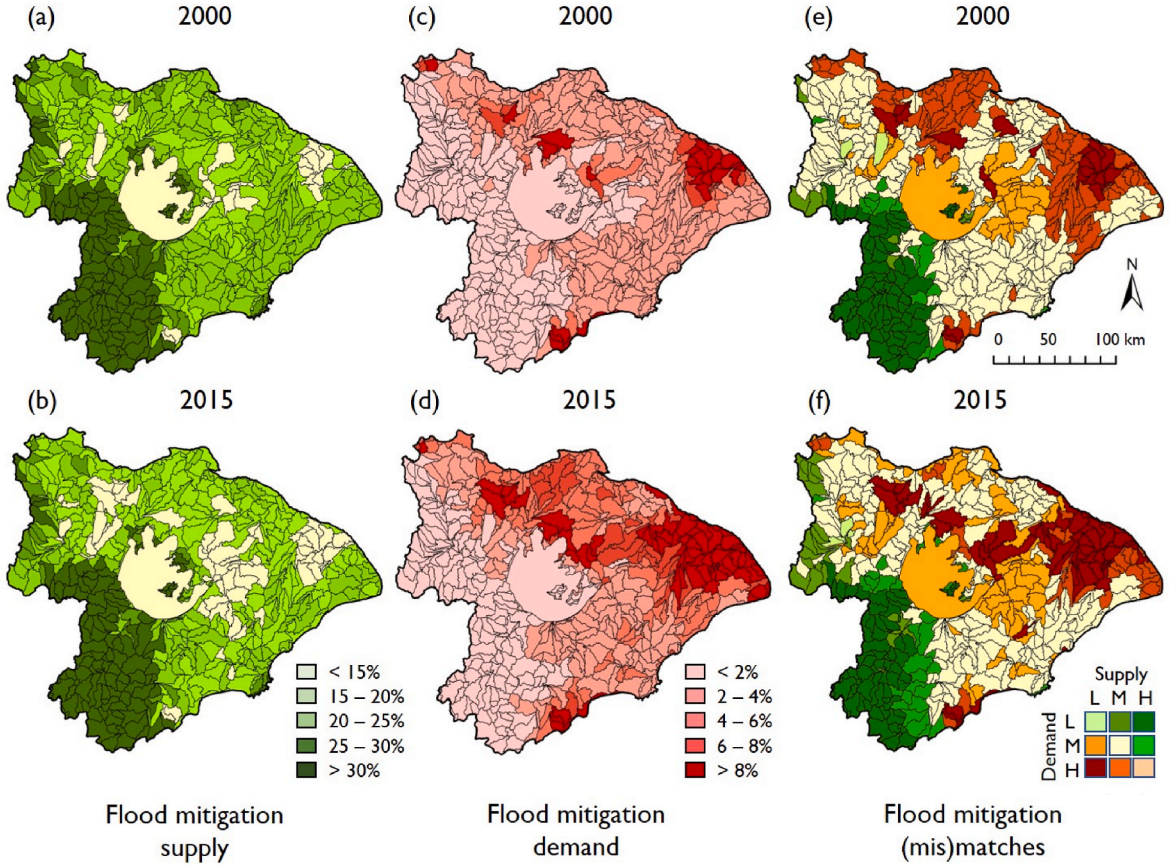

Fig. 4. Flood mitigation supply and demand in 2000 and 2015 (L = low, M = medium, H = high).

characterized by high or low supply and high or low demand were designated HH, HL, LH, and LL as described above. Although LL and HH regions covered less than 1% of the entire basin in both years, LH regions accounted for 5% and 14% of the basin territory in 2000 and 2015, representing a three-fold increase over a 15-year period. The LH regions corresponded closely to rapidly growing urban areas of the northeast, where flood risks and damages were notably higher than the other parts of the TLB. Had these areas been flooded in 2015, more than 40% of the population and gross domestic product would have been potentially affected. Regions of low supply and moderate demand also increased, by an average of 3% annually between 2000 and 2015. These regions, most of which were clustered near the center of the basin, were primarily comprised of croplands and water bodies. On the contrary, HL regions decreased in area from 15% to 12% of the basin territory during the same period. These were mostly on the eastern side of the sparsely populated low mountainous zone in the southwest.

3.3. Urbanization and land use effects on water purification supply and demand

The fitting analyses revealed a moderately decreasing trend of WP_S as urbanization transitioned from a low to high level (Fig. 5*a*, 5*b*, and 5*c*). In comparison, WP_D was the highest in agricultural sub-basins with moderate GDP and population density (Fig. 5*g* and 5*h*). Urban expansion, which mostly resulted from encroachment onto croplands, significantly decreased WP_D in these agricultural sub-basins (Fig. 5*i*). As a result, the level of urbanization was high in LL sub-basins, where urban land covered more than 60% of the area, but it covered no more than 20% of the area in the other sub-basins (Fig. 5*m*, 5*n*, and 5*o*).

There was a statistically significant increasing trend of WP_D and a less significant decreasing trend of WP_S as the proportion of croplands increased in the sub-basins (Fig. 5*d* and 5*j*). The magnitude of the decrease of WP_S and the increase of WP_D was greater as the proportion of croplands increased from a low to moderate level than from a moderate to high level. On average, 20% of the total nitrogen loading was exported into the water, while 80% of the nitrogen loading should be intercepted for protection of water quality in sub-basins with only croplands. Croplands made up about 80% of the total area in sub-basins with high WP_D, but they covered only 20% of the area in sub-basins with low WP_D (Fig. 5*p*).

In contrast, WP_S increased but WP_D decreased with an increasing proportion of woodland in the sub-basins (Fig. 5*e* and 5*k*). Moreover, woodland was more effective in improving WP_S while reducing WP_D as the proportion of woodland increased from a moderate to high level than from a low to moderate level. WP_S reached 90% of the total nitrogen loading while WP_D dropped to zero as woodland coverage surpassed 90% of sub-basin territory. Woodland dominated HL sub-basins where coverage averaged about 80%, but there was little or no woodland in the other sub-basins (Fig. 5*q*).

Open water covered a very small area of all the four types of sub-basins (Fig. 5*r*). The proportion of open water was not associated with WP_S, but it was negatively associated with WP_D (Fig. 5*f* and 5*l*). Overall, GDP and population density were not directly linked with WP_S and WP_D ($R^2 < 0.14$). Although the proportion of each land use had a strong association with WP_D ($R^2 > 0.57$), there was a weak influence of any one type of land use on WP_S ($R^2 < 0.34$). This implies that land use composition is crucial to WP_D, but that configuration of multiple land uses likely plays a more important role in determining WP_S at the sub-basin scale.

3.4. Urbanization and land use effects on flood mitigation supply and demand

FM_S decreased sharply at low levels of urbanization, but the rate

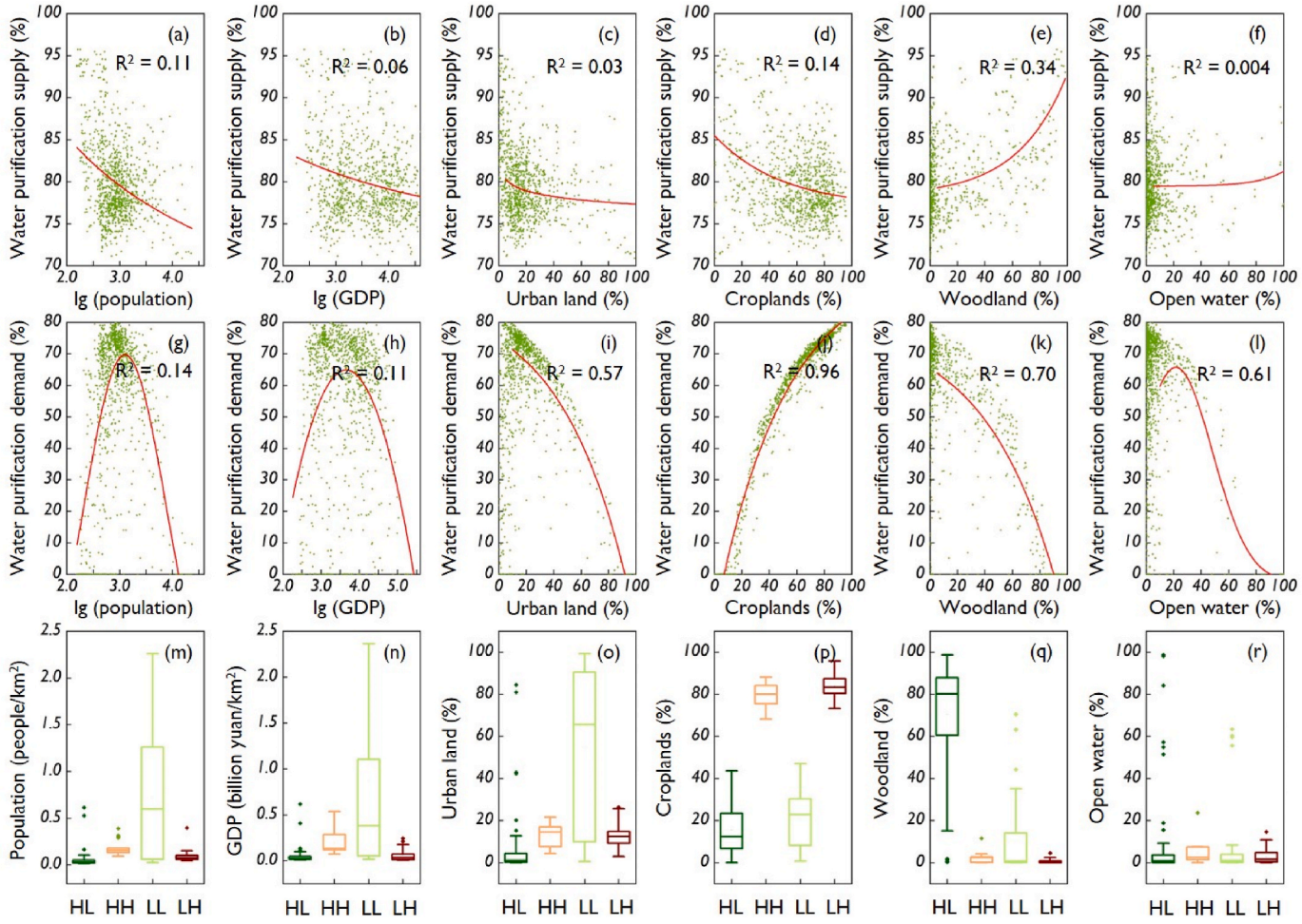

Fig. 5. Urbanization and land use effects on water purification supply and demand in the TLB.

moderated substantially as urbanization increased to moderate and high levels (Fig. 6*a*, 6*b*, and 6*c*). FM_D, on the other hand, was initially low but increased dramatically as population density surpassed 1000 people per square kilometer (Fig. 6*g*), or as GDP surpassed 100 million yuan per square kilometer (Fig. 6*h*), or as urban area surpassed 20% of sub-basin territory (Fig. 6*i*). Only 5% of surface runoff was reduced in urban areas, and the vulnerability of highly urbanized sub-basins to flooding approached 70% (Fig. 6*c* and 6*i*). Also as depicted in Fig. 6*m*, 6*n*, and 6*o*, the level of urbanization was significantly higher in LH sub-basins as compared to the other sub-basins.

The impact of an increase of croplands on FM_S and FM_D varied depending on how croplands interacted with other land uses in the sub-basins (Fig. 6*d* and 6*j*). FM_S decreased but FM_D increased with the expansion of croplands in wooded sub-basins located in the low mountains of the TLB. In contrast, FM_S increased but FM_D decreased as more croplands were conserved or reclaimed in urbanized sub-basins. Moreover, both FM_S and FM_D changed more drastically as the proportion of croplands increased from a low to moderate level, but a further increase in croplands to a high level resulted in only mild additional changes. Agricultural sub-basins entirely comprised of croplands could generally reduce 25% of surface runoff, while constraining vulnerability to floods to less than 10% of the maximum value. Croplands had only moderate influences on FM_S and FM_D, and thus there were no significant differences in the distribution of croplands among the four types of sub-basins (Fig. 6*p*).

The rate of increase of FM_S accelerated with an increasing proportion of woodland in the sub-basins. More than 80% of surface runoff was reduced in sub-basins covered solely by woodland, and the vulnerability of these wooded sub-basins to flooding became negligible (Fig. 6*e* and 6*k*). On average, woodland covered 60–70% of the total area in sub-basins with high FM_S, but it covered less than 5% of the area in sub-basins with low FM_S (Fig. 6*q*). Open water exhibited low FM_S and FM_D (Fig. 6*f* and 6*l*). Over 80% of the total area was open water in sub-basins with low FM_S and low FM_D (Fig. 6*r*). As indicated by the R^2 values in Fig. 6*a-l*, FM_S had a strong association with different land uses at the sub-basin scale, but FM_D increased primarily as a result of urban expansion ($R^2 = 0.74$) accompanied by population growth ($R^2 = 0.93$) and economic development ($R^2 = 0.81$).

4. Discussion

4.1. Comparisons of the findings with other case studies

In this study, hydrologic ecosystem services (also known as water-related ecosystem services) were found sensitive to rapid urbanization processes, such as urban land expansion and socio-economic development on a basin-wide scale. Several other studies also observed compromised hydrologic services in the TLB as it is developed into a highly urbanized basin over the past few decades. As estimated by Xu et al. (2016), two-thirds of the TLB have experienced degradation of water purification and water retention services during 1985–2010. Qiao et al. (2019) also found that rapid urban expansion in the TLB has led to dramatically decreased flood storage capacity of croplands over the same period. Similar to these findings in the TLB, water purification service in the Xiangjiang River Basin of southern China was declined as evidenced with significant increases in nitrogen and phosphorus export

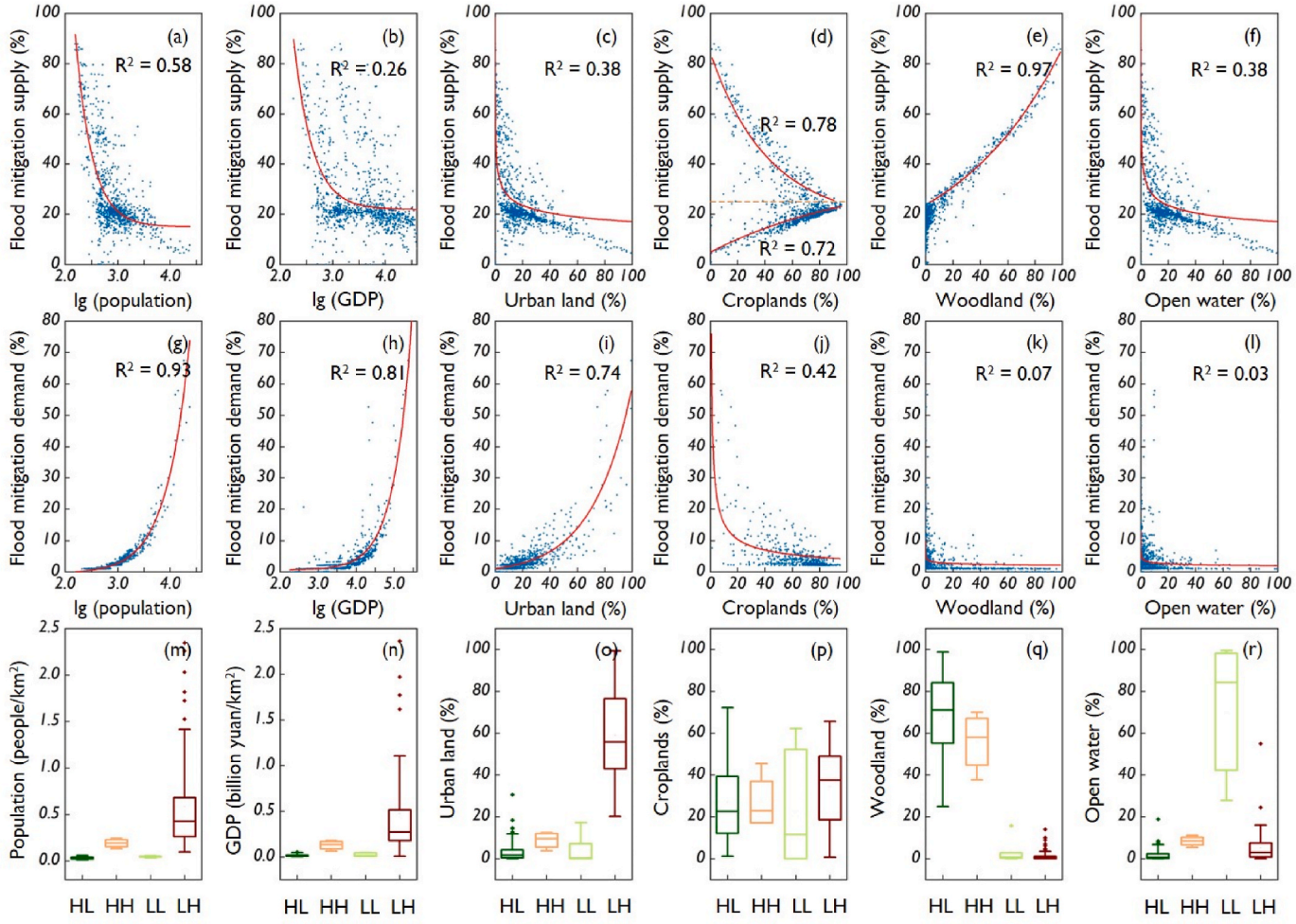

Fig. 6. Urbanization and land use effects on flood mitigation supply and demand in the TLB.

due to rapid urban expansion and agricultural intensification during 2000–2015 (Liang et al., 2021). Another case study in the Dianchi Lake Basin of China likewise revealed a notable increase in nitrogen export with predicted urban growth and losses of croplands and natural habitat between 2015 and 2035 (Wang et al., 2021).

In addition to decreased supply of hydrologic ecosystem services, our study observed intensified spatial mismatches between supply of and demand for water purification and flood mitigation services in the rapidly urbanizing TLB (Figs. 3 and 4). This result was verified by Li et al. (2016), in which they found a declined supply-demand ratio for a number of ecosystem services (including water purification and flood regulation) in the TLB with rapid urbanization between 2000 and 2010. Cao et al. (2021) concluded with similar findings for the Baiyangdian Basin of northern China that urbanization has been a major driver of increased deficiencies in ecosystem services supply to meet societal demand during 1980–2015. For flood regulation service in this Baiyangdian Basin, Li et al. (2022) also observed an intensified supply-demand imbalance with a 28% decrease in supply-demand ratio from 1990 to 2018 due primarily to rapid urbanization. For water purification service in another rapidly urbanizing basin on the Tibetan Plateau, the demand exceeded supply by 45% as of 2019, and the increase of water pollution from urban areas was discovered to be the main reason for such imbalance (Xia et al., 2022).

As illustrated in Figs. 5 and 6, the supply of and demand for hydrologic ecosystem services were significantly associated with socio-economic and land use factors at the sub-basin scale. This implied that urbanization could affect supply and demand dynamics of hydrologic services through changes in land use and socio-economic status. Several other studies in the TLB also revealed strong associations between nitrogen export and landscape characteristics, including land use composition (e.g., percentage of croplands and forest land) and spatial configuration (e.g., edge density and number of forest patches) (Bai et al., 2020; Wang et al., 2022). By taking two rapidly urbanizing basins of northwestern Oregon, USA as examples, Hoyer and Chang (2014) showed similar results that nutrient export and retention were overwhelmingly driven by land cover, as they found reduced nitrogen export due to losses of croplands from urban expansion while increased retention of nutrients with installation of riparian buffer strips. As to flood regulation service, the proportion of urban area was identified as the most important factor to influence its supply-demand ratio in the Baiyangdian Basin (Li et al., 2022), a result similar to what we have discovered in the TLB.

4.2. *Strengths and constraints of the ES supply and demand models*

As defined by Villamagna et al. (2013) and Wolff et al. (2015), the demand for regulatory ecosystem services is represented by the amount of regulation required to maintain desirable environmental conditions. In the case of nitrogen and water purification, WP_D can be quantified as the amount of non-point sourced nitrogen loading that ought to be reduced by terrestrial ecosystems such as woodland and grassland for maintenance of desirable surface water quality. Thus the key to quantifying WP_D was to estimate the allowable amount of nitrogen released in each sub-basin, which in our model was a function of water yield

multiplied by the maximum concentration of nitrogen according to the relevant water quality standard. Our model has three major advantages for quantifying WP_D. First, WP_D is measured as the difference between total and allowable nitrogen loading, while WP_S equals the reduction of nitrogen loading. This makes WP_D and WP_S directly comparable with the same unit of measurement. Second, the model provides spatially explicit estimates of WP_D and WP_S for each sub-basin, and this reveals spatial matches and mismatches between WP_D and WP_S across the larger region of interest. Third, the model is flexible in quantifying WP_D as the allowable amount of nitrogen loading varies with the threshold concentration of nitrogen under different water quality standards. The model can consequently be employed to explore the dynamics of WP_D in response to alternative water protection goals.

The demand for flood mitigation service (FM_D) can be defined as the vulnerability of an area to flood damage (Nedkov & Burkhard, 2012). In the previous studies, FM_D was determined by using various sources of topographic, demographic, and economic data from local authorities (Wang et al., 2019). As a result, urban and agricultural areas in floodplains were identified as the most vulnerable places with the highest FM_D (Vallecillo et al., 2020). Shen et al. (2019; 2021) proposed that FM_D could be alternatively quantified as the direct economic loss caused by floods, which depends on the intensity of land use and flood depth. We also quantified FM_D as flood damage values, but we also considered both economic losses and human mortalities. Thus the populous and prosperous urban areas exhibited high FM_D in our study. Although we estimated runoff retention and flood damage values as measurements of FM_S and FM_D, these two indicators do not share the same unit of measurement. We consequently compared FM_S with FM_D by dividing each form of measurement into low, medium, and high levels that could be color-coded as depicted in Fig. 3*f* and 4*f*.

The TLB is characterized by flat terrain with surface water flows that have been extensively reshaped by dams, dikes, and ditches. It was difficult to delineate sub-basins with accurate water flow directions and quantities; accordingly, our model quantified FM_S and FM_D separately for each sub-basin without considering transboundary impacts. But in fact, it is important to unravel hydrological connections between upstream and downstream areas in quantifying flow-dependent ecosystem services (Goldenberg et al., 2017). As recommended by Stürck et al. (2014), future studies should quantify FM_D on the basis of aggregated flood damage within and downstream of each sub-basin in relation to the extent of upstream service provisioning area. Similar studies should quantify WP_D by taking into account the inflows of runoff and nitrogen from upstream sub-basins.

4.3. Policy implications of the results

Based on the findings of this study, agricultural areas were the primary contributors to excessive nitrogen export into water bodies (Fig. 3), and they should be appropriately managed for improving water quality in the TLB. Large urban areas, such as the cities of Shanghai, Suzhou, Wuxi, and Changzhou, were concentrated in the northeastern part of the basin with relatively high vulnerability to flood risks (Fig. 4), thus urban flood control should be prioritized for these rapidly expanding cities. In comparison, the forested mountains in the southwest of the TLB were the primary provisioning areas for both water purification and flood mitigation services (Figs. 3 and 4). These ecological source areas deserve strict protection from human disturbances (e.g., urban and agricultural development) through the implementation of ecological red line policies, some of which have already been implemented at varied stages.

More specifically, we propose the following several non-exclusive land management measures to improve water purification and flood mitigation services for ultimately achieving the Sustainable Development Goals (e.g., SDG-6 of clean water and sanitation, and SDG-11 of sustainable cities and communities) in the TLB. First, because WP_S and WP_D were most sensitive to the increase of fragmented cropland patches, aggregation of croplands would be of great benefit in reducing the impact of agricultural activities on water purification. In addition, 80% of nitrogen loading from agricultural areas should be reduced through better management of fertilization, as well as adding buffer strips to protect water quality. This is in particular relevant for the identified supply-demand mismatch locales. Second, croplands on steep, easily erodible slopes should be converted to woodlands, as well as simultaneously protected from urban expansion for enhancing FM_S and reducing FM_D, and thus strike a balance between the supply and demand for each service. Third, degraded woodlands in key areas such as hillsides and riparian zones should be restored as an ecologically sensitive means to effectively reduce nitrogen loading and peak flow and thus mitigate the supply gap of services. Fourth, the proportion of urban land in any rapidly urbanizing sub-basin should be controlled so that it does not exceed the 20% threshold above which sharp increases in FM_D become evident. For the urban area, the implementation of green infrastructures, such as bioretention ponds, green roofs, and permeable pavement would contribute to urban flooding reduction (Maragno et al., 2018). Although the spatial configuration of mixed land uses was not explicitly tested in this study, it might be as important as land use composition in influencing WP_S (Qiu, 2019; Qiu & Turner, 2015; Rieb & Bennett, 2020). This implied more opportunities for water pollution control through optimizing the size, shape, location, and density of different land parcels in the TLB, especially when the capacity to modify landscape composition is limited.

5. Conclusions

This study developed two integrated models for quantifying the supply and demand dynamics of water purification and flood mitigation services in response to rapid urban expansion in the TLB. According to our analyses, the low mountains of the southwest TLB were the primary service provisioning areas for WP_S and FM_S. Urban and rural settlements in the northeast were the most vulnerable places to flood damage with high FM_D. While agricultural areas exhibited high WP_D as the dominant contributor to nitrogen export. Both WP_S and WP_D decreased due to loss of croplands to urban expansion between 2000 and 2015. In comparison, FM_S decreased but FM_D dramatically increased as urban area surpassed 20% of sub-basin territory. Overall, land use composition had a strong association with WP_D and FM_S, but that configuration of multiple land uses might play a critical role in influencing WP_S. In addition, FM_D increased primarily because of urban expansion, population growth, and economic development in the TLB. To improve these two ecosystem services, we propose to control urban sprawl, to aggregate cropland patches, and to restore riparian areas in the future land management practices.

Declaration of competing interest

The authors declare that they have no known competing financial interests or personal relationships that could have appeared to influence the work reported in this paper.

Acknowledgments

The authors are grateful to the anonymous reviewers and editors for their valuable comments and suggestions. This research was supported by the National Natural Science Foundation of China (42271304, 42271106, 41971230); the Jiangsu Talent Program for Innovation and Entrepreneurship (JSSCBS20210282); the Strategic Priority Research Program of the Chinese Academy of Sciences (XDA23020201); the Basic Research Program of Jiangsu Province (BK20170725); the NAU-MSU Joint Research Project (2017-AH-10); and the Program of Introducing Talents of Discipline to Universities (B17024).

References

Bai, Y., Chen, Y., Alatalo, J., et al. (2020). Scale effects on the relationships between land characteristics and ecosystem services – a case study in Taihu Lake Basin, China. *Science of the Total Environment, 716*, Article 137083.

Baró, F., Haase, D., Gómez-Baggethun, E., et al. (2015). Mismatches between ecosystem services supply and demand in urban areas: A quantitative assessment in five European cities. *Ecological Indicators, 55*, 146–158.

Baró, F., Palomo, I., Zulian, G., et al. (2016). Mapping ecosystem service capacity, flow and demand for landscape and urban planning: A case study in the barcelona metropolitan region. *Land Use Policy, 57*, 405–417.

Burkhard, B., Kroll, F., Nedkov, S., et al. (2012). Mapping ecosystem service supply, demand and budgets. *Ecological Indicators, 21*, 17–29.

Cao, T., Yi, Y., Liu, H., et al. (2021). The relationship between ecosystem service supply and demand in plain areas undergoing urbanization: A case study of China's Baiyangdian Basin. *Journal of Environmental Management, 289*, Article 112492.

Chen, J., Jiang, B., Bai, Y., et al. (2019). Quantifying ecosystem services supply and demand shortfalls and mismatches for management optimization. *Science of the Total Environment, 650*, 1426–1439.

Chen, D., Li, J., Yang, X., et al. (2020). Quantifying water provision service supply, demand and spatial flow for land use optimization: A case study in the YanHe watershed. *Ecosystem Services, 43*, Article 101117.

Cui, F., Tang, H., Zhang, Q., et al. (2019). Integrating ecosystem services supply and demand into optimized management at different scales: A case study in hulunbuir, China. *Ecosystem Services, 39*, Article 100984.

Daily, G., Soderquist, T., Aniyar, S., et al. (2000). The value of nature and the nature of value. *Science, 289*, 395–396.

Goldenberg, R., Kalantari, Z., Cvetkovic, V., et al. (2017). Distinction, quantification and mapping of potential and realized supply-demand of flow-dependent ecosystem services. *Science of the Total Environment, 593–594*, 599–609.

González-García, A., Palomo, I., González, J., et al. (2020). Quantifying spatial supply-demand mismatches in ecosystem services provides insights for land-use planning. *Land Use Policy, 94*, Article 104493.

Hou, Y., Ding, S., Chen, W., et al. (2020). Ecosystem service potential, flow, demand and their spatial associations: A comparison of the nutrient retention service between a human- and a nature-dominated watershed. *Science of the Total Environment, 748*, Article 141341.

Hoyer, R., & Chang, H. (2014). Assessment of freshwater ecosystem services in the Tualatin and Yamhill basins under climate change and urbanization. *Applied Geography, 53*, 402–416.

Huang, Q., Yin, D., He, C., et al. (2020). Linking ecosystem services and subjective well-being in rapidly urbanizing watersheds: Insights from a multilevel linear model. *Ecosystem Services, 43*, Article 101106.

Huizinga, J., Moel, H., & Szewczyk, W. (2017). Global flood depth-damage functions: Methodology and the database with guidelines. *EUR 28552 EN*. https://doi.org/10.2760/16510

Jonkman, S. (2007). *Loss of life estimation in flood risk assessment: Theory and applications. PhD thesis*. Delft University of Technology.

Kroll, F., Müller, F., Haase, D., et al. (2012). Rural-urban gradient analysis of ecosystem services supply and demand dynamics. *Land Use Policy, 29*, 521–535.

Liang, J., Li, S., Li, X., et al. (2021). Trade-off analyses and optimization of water-related ecosystem services (WRESs) based on land use change in a typical agricultural watershed, southern China. *Journal of Cleaner Production, 279*, Article 123851.

Li, H., Chen, W., Yang, G., et al. (2013). Reduction of nitrogen and phosphorus emission and zoning management targeting at water quality of lake or reservoir systems: A case study of shahe reservoir within tianmuhu reservoir area. *Journal of Lake Sciences, 25*, 785–798 (in Chinese).

Li, J., Fang, Z., Zhang, J., et al. (2022). Mapping basin-scale supply-demand dynamics of flood regulation service – a case study in the Baiyangdian Lake Basin, China. *Ecological Indicators, 139*, Article 108902.

Li, F., Guo, S., Li, D., et al. (2020). A multi-criteria spatial approach for mapping urban ecosystem services demand. *Ecological Indicators, 112*, Article 106119.

Li, J., Jiang, H., Bai, Y., et al. (2016). Indicators for spatial-temporal comparisons of ecosystem service status between regions: A case study of the Taihu River Basin, China. *Ecological Indicators, 60*, 1008–1016.

Lin, J., Huang, J., Prell, C., et al. (2021). Changes in supply and demand mediate the effects of land-use change on freshwater ecosystem services flows. *Science of the Total Environment, 763*, Article 143012.

Liu, J., Kuang, W., Zhang, Z., et al. (2014). Spatiotemporal characteristics, patterns and causes of land use changes in China since the late 1980s. *Acta Geographica Sinica, 69*, 3–14 (in Chinese).

Maragno, D., Gaglio, M., Robbi, M., et al. (2018). Fine-scale analysis of urban flooding reduction from green infrastructure: An ecosystem services approach for the management of water flows. *Ecological Modelling, 386*, 1–10.

Ma, S., Smailes, M., Zheng, H., et al. (2019). Who is vulnerable to ecosystem service change? Reconciling locally disaggregated ecosystem service supply and demand. *Ecological Economics, 157*, 312–320.

Nedkov, S., & Burkhard, B. (2012). Flood regulating ecosystem services – mapping supply and demand, in the Etropole municipality, Bulgaria. *Ecological Indicators, 21*, 67–79.

Pan, Z., He, J., Liu, D., et al. (2021). Ecosystem health assessment based on ecological integrity and ecosystem services demand in the Middle Reaches of the Yangtze River Economic Belt, China. *Science of the Total Environment, 774*, Article 144837.

Peng, J., Tian, L., Liu, Y., et al. (2017). Ecosystem services response to urbanization in metropolitan areas: Thresholds identification. *Science of the Total Environment, 607–608*, 706–714.

Peng, J., Wang, X., Liu, Y., et al. (2020). Urbanization impact on the supply-demand budget of ecosystem services: Decoupling analysis. *Ecosystem Services, 44*, Article 101139.

Peng, J., Wei, H., Wu, W., et al. (2018). Storm flood disaster risk assessment in urban area based on the simulation of land use scenarios: A case of maozhou watershed in shenzhen city. *Acta Ecologica Sinica, 38*, 3741–3755 (in Chinese).

Qiao, X., Gu, Y., Zou, C., et al. (2019). Temporal variation and spatial scale dependency of the trade-offs and synergies among multiple ecosystem services in the Taihu Lake Basin of China. *Science of the Total Environment, 651*, 218–229.

Qiu, J. (2019). Effects of landscape pattern on pollination, pest control, water quality, flood regulation, and cultural ecosystem services: A literature review and future research prospects. *Current Landscape Ecology Reports, 4*, 113–124.

Qiu, J., & Turner, M. (2013). Spatial interactions among ecosystem services in an urbanizing agricultural watershed. *Proceedings of the National Academy of Sciences, 110*, 12149–12154.

Qiu, J., & Turner, M. (2015). Importance of landscape heterogeneity in sustaining hydrologic ecosystem services in an agricultural watershed. *Ecosphere, 6*, 1–19.

Rieb, J., & Bennett, E. (2020). Landscape structure as a mediator of ecosystem service interactions. *Landscape Ecology, 35*, 2863–2880.

Sharp, R., Tallis, H., Ricketts, T., et al. (2018). *InVEST 3.5.0 user's guide. The natural capital Project*. Stanford University, University of Minnesota, The Nature Conservancy, and World Wildlife Fund.

Shen, J., Du, S., Huang, Q., et al. (2019). Mapping the city-scale supply and demand of ecosystem flood regulation services – a case study in Shanghai. *Ecological Indicators, 106*, Article 105544.

Shen, J., Du, S., Ma, Q., et al. (2021). A new multiple return-period framework of flood regulation service – applied in Yangtze River basin. *Ecological Indicators, 125*, Article 107441.

Shi, Y., Shi, D., Zhou, L., et al. (2020). Identification of ecosystem services supply and demand areas and simulation of ecosystem service flows in Shanghai. *Ecological Indicators, 115*, Article 106418.

Shi, P., Yuan, Y., & Chen, J. (2001). The effect of land use on runoff in Shenzhen City of China. *Acta Ecologica Sinica, 21*, 1041–1050 (in Chinese).

Stürck, J., Poortinga, A., & Verburg, P. (2014). Mapping ecosystem services: The supply and demand of flood regulation services in Europe. *Ecological Indicators, 38*, 198–211.

Stürck, J., Schulp, C., & Verburg, P. (2015). Spatio-temporal dynamics of regulating ecosystem services in Europe – the role of past and future land use change. *Applied Geography, 63*, 121–135.

Sun, X., Tang, H., Yang, P., et al. (2020). Spatiotemporal patterns and drivers of ecosystem service supply and demand across the conterminous United States: A multiscale analysis. *Science of the Total Environment, 703*, Article 135005.

Taihu Basin Authority of Ministry of Water Resources. (2015). *The 2015 Health Status Report of Taihu Lake,* (pp. 1–24) (in Chinese).

Taihu Basin Authority of Ministry of Water Resources. (2020). *The 2020 water resources bulletin of Taihu basin & southeast rivers* (pp. 1–24) (in Chinese).

Tao, Y., Tao, Q., Sun, X., et al. (2022). Mapping ecosystem service supply and demand dynamics under rapid urban expansion: A case study in the Yangtze River Delta of China. *Ecosystem Services, 56*, Article 101448.

Tao, Y., Wang, H., Ou, W., et al. (2018). A land-cover-based approach to assessing ecosystem services supply and demand dynamics in the rapidly urbanizing Yangtze River Delta region. *Land Use Policy, 72*, 250–258.

Vallecillo, S., Kakoulaki, G., Notte, A., et al. (2020). Accounting for changes in flood control delivered by ecosystems at the EU level. *Ecosystem Services, 44*, Article 101142.

Villamagna, A., Angermeier, P., & Bennett, E. (2013). Capacity, pressure, demand, and flow: A conceptual framework for analyzing ecosystem service provision and delivery. *Ecological Complexity, 15*, 114–121.

Wang, Y., Atallah, S., & Shao, G. (2017). Spatially explicit return on investment to private forest conservation for water purification in Indiana, USA. *Ecosystem Services, 26*, 45–57.

Wang, R., Bai, Y., Alatalo, J., et al. (2021). Impacts of rapid urbanization on ecosystem services under different scenarios – a case study in Dianchi Lake Basin, China. *Ecological Indicators, 130*, Article 108102.

Wang, Y., Yang, G., Li, B., et al. (2022). Measuring the zonal responses of nitrogen output to landscape pattern in a flatland with river network: A case study in Taihu Lake Basin, China. *Environmental Science and Pollution Research, 29*, 34624–34636.

Wang, L., Zheng, H., Wen, Z., et al. (2019). Ecosystem service synergies/trade-offs informing the supply-demand match of ecosystem services: Framework and application. *Ecosystem Services, 37*, Article 100939.

Wei, H., Liu, H., Xu, Z., et al. (2018). Linking ecosystem services supply, social demand and human well-being in a typical mountain-oasis-desert area, Xinjiang, China. *Ecosystem Services, 31*, 44–57.

Wen, H., Zhou, J., Li, M., et al. (2011). Estimation of non-point soluble nitrogen and phosphorus pollutant loads in the drainage area of Liuxi River Reservoir. *Research of Environmental Sciences, 24*, 387–394 (in Chinese).

Wolff, S., Schulp, C., & Verburg, P. (2015). Mapping ecosystem services demand: A review of current research and future perspectives. *Ecological Indicators, 55*, 159–171.

Wu, X., Liu, S., Zhao, S., et al. (2019). Quantification and driving force analysis of ecosystem services supply, demand and balance in China. *Science of the Total Environment, 652*, 1375–1386.

Xia, P., Chen, B., Gong, B., et al. (2022). The supply and demand of water purification service in an urbanizing basin on the Tibetan Plateau. *Landscape Ecology, 37*, 1937–1955.

Xu, Z., Wei, H., Dong, X., et al. (2020). Evaluating the ecological benefits of plantations in arid areas from the perspective of ecosystem service supply and demand-based on emergy analysis. *Science of the Total Environment, 705*, Article 135853.

Xu, X., Yang, G., Tan, Y., et al. (2016). Ecological risk assessment of ecosystem services in the Taihu Lake Basin of China from 1985 to 2020. *Science of the Total Environment, 554–555*, 7–16.

Xu, Q., Yang, R., Zhuang, D., et al. (2021). Spatial gradient differences of ecosystem services supply and demand in the Pearl River Delta region. *Journal of Cleaner Production, 279*, Article 123849.

Xu, S., Zhang, Y., Dou, M., et al. (2017). Spatial distribution of land use change in the Yangtze River Basin and the impact on runoff. *Progress in Geography, 36*, 426–436 (in Chinese).

Zhai, T., Wang, J., Jin, Z., et al. (2020). Did improvements of ecosystem services supply-demand imbalance change environmental spatial injustices? *Ecological Indicators, 111*, Article 106068.